Talanta 89 (2012) 136–141

Contents lists available at SciVerse ScienceDirect

Talanta

journal homepage: www.elsevier.com/locate/talanta

Simultaneous electrochemical determination of dopamine and ascorbic acid using AuNPs@polyaniline core–shell nanocomposites modified electrode

Limin Yang, Shufeng Liu, Qixiu Zhang, Feng Li*

College of Chemistry and Molecular Engineering, Qingdao University of Science and Technology, Qingdao 266042, People's Republic of China

ARTICLE INFO

Article history:
Received 22 August 2011
Received in revised form 1 December 2011
Accepted 1 December 2011
Available online 8 December 2011

Keywords:
AuNPs@PANI
Core–shell
Dopamine
Ascorbic acid
Simultaneous determination

ABSTRACT

A simple and effective strategy was proposed for synthesis of AuNPs@polyaniline (AuNPs@PANI) core–shell nanocomposites. AuNPs@PANI nanocomposites were prepared by one-step chemical oxidative polymerization of aniline using chloroaurate acid as the oxidant and AuNPs as the seeds. The synthesized AuNPs@PANI nanocomposites were characterized with transmission electron microscope and UV–vis absorption spectra. Cyclic voltammetric experiments indicated that AuNPs@PANI nanocomposites showed excellent electroactivity in neutral and even alkaline solution. The obtained AuNPs@PANI nanocomposites-modified electrode was fabricated to simultaneously determine dopamine (DA) and ascorbic acid (AA) by differential pulse voltammetry. The separation between the two peak potentials of DA and AA oxidation is 236 mV. The catalytic peak currents were linearly with the concentrations of DA and AA in the range of 10–1700 and 20–1600 μM with correlation coefficients of 0.9997 and 0.9998, respectively. The detection limits for DA and AA were 5 and 8 μM, respectively.

1. Introduction

Dopamine (DA) and ascorbic acid (AA) are chemicals with significant roles in regulation of human metabolism as well as in the central nervous and renal systems. Both species are vitally related to the diagnosis of various kinds of diseases. For example, abnormal levels of DA have become the diagnostic criteria to Parkinson's disease, Schizophrenia and neuroendocrine disorder [1,2]. Similarly, AA is known to take part in several biological reactions and its content is related to cancer and hepatic diseases [3]. Since they usually coexist in real biological matrices, the development of a selective and sensitive method for their simultaneous determination is highly desirable for analytical and diagnostic applications. Owing to the overlap of their voltammetric responses, it is often very difficult to achieve their simultaneous determination based on electrochemical methods [4,5]. To solve this issue, some efforts have been developed to modify the electrode with metal nanoparticles [6–8], carbon nanotube [9], inorganic redox mediators [10] and conducting polymers [11–13]. Among them, conducting polymers have received considerable attention because of their easy preparation, good biocompatibility and stability.

Among the known conducting polymers, PANI is one of the most important conducting polymers due to its remarkable electrical, electrochemical and optical properties as well as good environmental stability [14]. These above advantages make PANI quite suitable as an electronic material, especially in the fabrication of sensors or biosensors [15–18]. However, PANI nearly has no electroactivity in media with pH >4 [19,20]. Since a neutral environment is usually required in the bioanalysis process, the rigorous condition for maintaining the electroactivity of PANI in acidic media in a large way restricts its application in bioengineering. Therefore, tremendous efforts have been invested to develop PANI with excellent redox activity at neutral pH environment [21–24].

The incorporation of metallic nanoparticles into conductive polymers is of great interest because of their strong electronic interactions between the nanoparticles and the polymer matrixes. It has been reported that the electrocatalytic properties of nanoparticles could be enhanced by the conductive polymeric matrixes. Additionally, the conductivity of the hybrid systems is largely improved [25]. Recently, several reports have been made on incorporating AuNPs into polymer matrixes to produce novel nanocomposite materials [26,27]. Wang and co-workers prepared PANI nanotubes and Au nanoplates simultaneously by mixing aniline and chloroauric acid hydrate in the presence of CTAB [28]. Using $(NH_4)_2S_2O_8$ as oxidant, AuNPs@PANI composites were obtained with the adsorption and *in situ* polymerization of aniline on the surface of AuNPs in the presence of sodium dodecylsulfate [29]. Peng and co-workers obtained PANI–Au nanocomposites with core–shell structure by direct oxidation of aniline using $HAuCl_4$ as the oxidant [30].

Herein, a facile strategy for synthesis of AuNPs@PANI nanocomposites was proposed by polymerization of aniline using AuNPs as the seeds and $HAuCl_4$ as the oxidant. Cyclic voltammetric

* Corresponding author. Fax: +86 532 84023927.
E-mail address: lifeng@qust.edu.cn (F. Li).

0039-9140/$ – see front matter © 2011 Elsevier B.V. All rights reserved.
doi:10.1016/j.talanta.2011.12.002

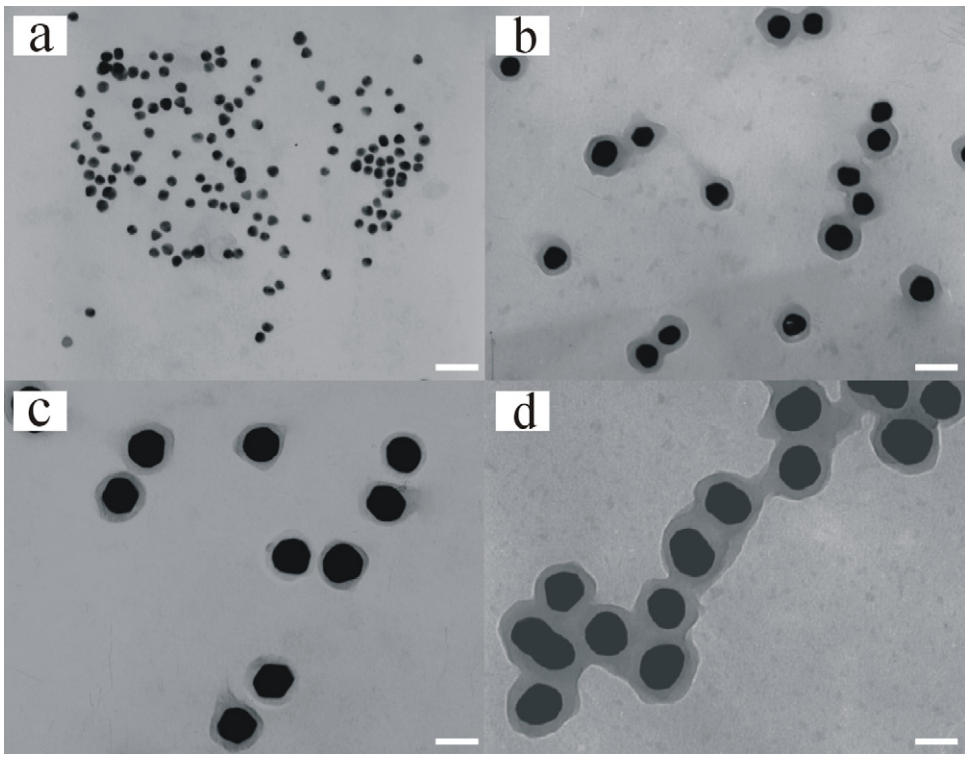

Fig. 1. TEM images of (a) AuNPs and typical products obtained with the following $HAuCl_4$-to-aniline molar ratios: (b) 0.25:1, (c) 0.5:1 and (d) 0.75:1. [Aniline] = 1.0 mM, [HCl] = 25 mM. Scale bar: 50 nm.

experiments proved that AuNPs@PANI nanocomposites had excellent electroactivity in neutral and even alkaline media. The excellent electrochemical catalytic activities towards DA and AA were achieved by the AuNPs@PANI nanocomposites modified glassy carbon electrode (GCE). The oxidation overpotentials of DA and AA significantly decreased and their oxidation peak currents dramatically increased at AuNPs@PANI modified GCE. Application to the analysis of real samples was also investigated.

2. Experimental

2.1. Chemicals

Chloroauric acid tetrahydate ($HAuCl_4{\cdot}4H_2O$) was supplied by Sinopharm Chemical Reagent Co., Ltd. Trisodium citrate and acetic acid (HAc) were purchased from Sigma–Aldrich. Chitosan (CS) with 98% deacetylation and an average molecular weight of 6×10^4 g mol^{-1} (Yuhuan Biomedical Corp., China) was used in this study. DA was purchased from Sigma–Aldrich. AA and sodium dodecyl sulfate (SDS) were from Tianjin Bodi Chemical Co. Ltd. Aniline monomer (purity 99.5%) was purchased from Tianjin Ruijinte Chemical Co. Ltd. Aniline was distilled into colorless under reduced pressure prior to use.

The 0.1 M phosphate buffer solutions (PBS) at various pH values were prepared by mixing the stock solutions of NaH_2PO_4 and Na_2HPO_4 and then adjusted with different amounts of 0.1 M NaOH or H_3PO_4. All other chemicals were of analytical grade and doubly distilled water (DDW) was used throughout this work.

2.2. Apparatus and instruments

Cyclic voltammetric (CV), electrochemical impedance spectroscopy (EIS) and amperometric measurements were performed with a CHI 660 D electrochemical analyzer (Shanghai CH Instrument Company, China). A conventional three-electrode system was used with bare glassy carbon electrode (GCE) or modified GCE as the working electrode, saturated calomel electrode (SCE) as reference electrode, and platinum wire as auxiliary electrode, respectively. Transmission electron microscopy (TEM) images were obtained using JEM–200EX transmission electron microscope with an accelerating voltage of 160.0 kV. The UV–vis absorption spectra of AuNPs and AuNPs@PANI were recorded on a Cary 50 Scan UV–vis spectrophotometer (Varian, USA) at room temperature.

2.3. Synthesis of AuNPs@PANI core–shell nanocomposites

AuNPs seeds were prepared by the conventional citrate reduction of $HAuCl_4$ in aqueous solution according to the literature [31]. Citrate-stabilized AuNPs (2.0 mL) were concentrated to a total of 20 μL after centrifugation at 12,000 rpm for 15 min. The isolated AuNPs were then added to a mixture of acidic aniline (3.0 mM, 5.0 mL) solution and SDS (15.0 mM, 5.0 mL). Different concentrations of $HAuCl_4$ (5.0 mL) solution were dropped into the above mixture under stirring at room temperature. The total volume of the final mixture was 15 mL, where [aniline] = 1.0 mM, [SDS] = 5.0 mM and [HCl] = 25.0 mM. The reaction mixture was incubated for 4 h under stirring to ensure complete polymerization. After that, the precipitate was centrifuged and washed several times with distilled water and ethanol. The final product was dried in vacuum at 40 °C for 24 h.

2.4. Preparation of the modified GCE

The GCE was carefully polished with 0.3 μm and 0.05 μm α-Al_2O_3 slurry, respectively, before each experiment, and followed by successive sonication in DDW and ethanol for 5 min. Then the GCE was thoroughly rinsed with water and dried at room temperature.

Firstly, 0.5% CS aqueous solution was prepared according to the previously reported procedure [32]. Briefly, 0.05 g CS flakes were dissolved in 10.0 mL 0.05 M HAc solution. After the undissolved

material was filtered, the pH was adjusted to 5.5 using 1.0 M NaOH. Then, 10.0 μL of the obtained CS solution was deposited on the pretreated electrode. The electrode was then placed under humid conditions for 4 h. After thoroughly rinsed by DDW, the obtained CS/GCE was immersed in AuNPs@PANI solutions for 6 h. The as-prepared electrode was denoted as AuNPs@PANI/CS/GCE.

2.5. Characterization

The synthesized AuNPs@PANI nanocomposites were characterized with TEM and UV–vis absorption spectroscopy. CV experiments were carried out in quiescent solutions with the scan rate of 50 mV s^{-1}. EIS experiments were performed in 1.0 mM $K_3Fe(CN)_6/K_4Fe(CN)_6$ (1:1) mixture containing 0.1 M KCl with the voltage frequencies ranging from 10^4 to 10^{-1} Hz.

3. Results and discussion

3.1. TEM of AuNPs@PANI core–shell nanocomposites

The structure of the prepared AuNPs@PANI was confirmed directly by TEM. As shown in Fig. 1, the synthesized AuNPs seeds showed a size of 13 nm (Fig. 1(a)). It could be seen that the polymerization growth of aniline by $HAuCl_4$ oxidation occurred around the AuNPs seeds and a core–shell structure of AuNPs@PANI composites was obtained. The dark spot and light coating in the TEM images represented the AuNPs and PANI, respectively. The morphology of AuNPs@PANI composites was found to change when the molar ratio of $HAuCl_4$-to-aniline varied. As shown in Fig. 1(b–c), the AuNPs inside the composites underwent a persistent growth when $HAuCl_4$ concentration increased. It has been reported that the PANI–Au composites could be obtained by direct oxidation of aniline using $HAuCl_4$ as the oxidant [30], where the obtained composites show a core–shell structure and the AuNPs are encapsulated by PANI of tetrahedron shape. Herein, the core–shell structure of AuNPs@PANI nanocomposites is attributed to the existence of AuNPs seeds and the product show an orbicular shape. The aniline could preferentially adsorb onto the surface of Au seeds by NH_2–Au interaction and offer suitable nucleation sites for the formed aniline oligomers during the polymerization process. As the reaction proceeds, the further gold deposition occurs on the AuNPs seeds and the formed PANI on the AuNPs surface provides a steric barrier against the further growth of AuNPs.

3.2. UV–vis spectra

Fig. 2 shows the UV–vis spectra of the prepared AuNPs and AuNPs@PANI. The AuNPs exhibit an absorption peak at 520 nm (Fig. 2(a)) [33]. As shown in Fig. 2, when the molar ratio of $HAuCl_4$ to aniline was 0.25:1, the absorption peak for the AuNPs shifted to about 532 nm (Fig. 2(b)). While the ratio was 0.5:1, a slight shift of the absorption peak to about 535 nm was observed (Fig. 2(c)). With molar ratio increased to 0.75:1, the absorption peak further red shifted to about 538 nm (Fig. 2(d)). This strongly indicated that the growth of AuNPs occurred during the polymerization of aniline. Results were consistent with those observed by TEM. As the concentration of $HAuCl_4$ increases, the polaron band at about 770 nm related to the absorption of PANI becomes broader and shifts to longer wavelengths. Since the absorption of the polaron band is strongly dependent on the molecular weight and protonation level of the PANI [34], this indicates a difference in molecular weight of the polymer with increasing $HAuCl_4$ concentration.

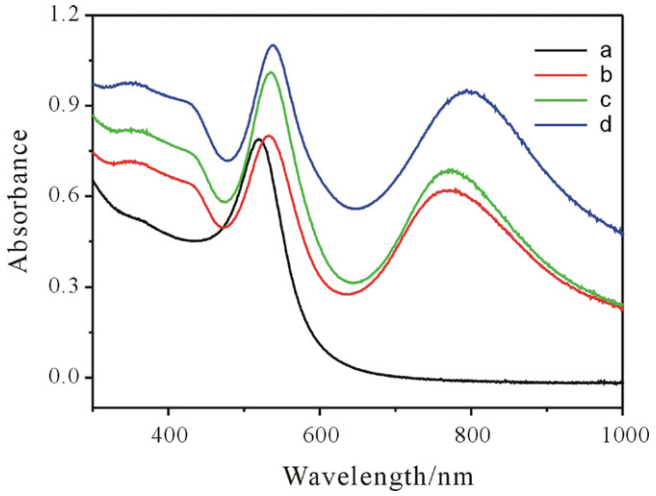

Fig. 2. UV–vis spectra of (a) AuNPs and typical products obtained with the following $HAuCl_4$-to-aniline molar ratios: (b) 0.25:1, (c) 0.5:1 and (d) 0.75:1.

3.3. Electroactivity of the AuNPs@PANI nanoparticles

Fig. 3 shows CVs of different electrodes in the potential range from −200 to 600 mV in phosphate buffer solution (pH 6.0) at a scan rate of 50 mV s^{-1}. No redox peaks appeared for bare GCE and CS/GCE (Fig. 3(a and b)). In contrast, a pair of well-defined redox peaks was observed for the AuNPs@PANI/CS/GCE with the anodic and cathodic potential of 163 mV and 195 mV, respectively. The peaks were attributed to the redox reaction of AuNPs@PANI. Therfore, AuNPs@PANI has been successfully immobilized on the electrode surface and showed remarkable redox behavior at neutral pH environment. The well redox behavior of AuNPs@PANI nanocomposites was attributed to the incorporation of AuNPs and was similar to results from Au NPs/PANI hybrid systems in neutral environment [25,35].

EIS was further employed to characterize the interface properties of the modified electrodes [36]. The typical results of AC impedance spectra of the bare GCE (a), CS/GCE (b), AuNPs@PANI/CS/GCE (c) were obtained in 0.1 M KCl containing 1.0 mM $Fe(CN)_6^{3-}$ and 1.0 mM $Fe(CN)_6^{4-}$ with the frequency ranging from 10^4 to 10^{-1} Hz (see Supplementary material Fig. S1). As can be seen, significant differences in the

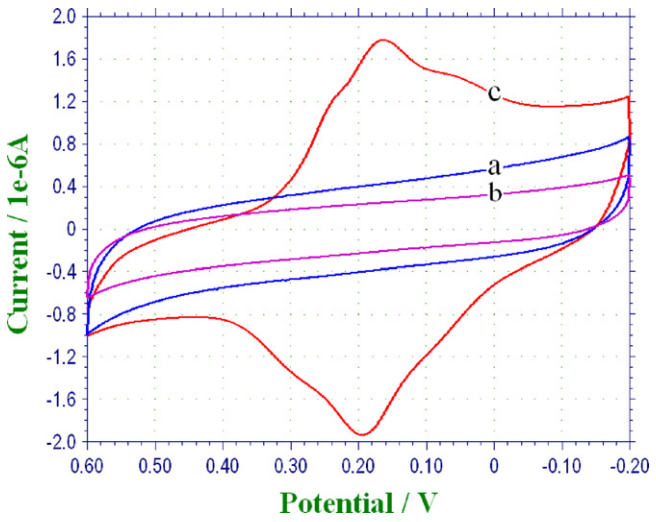

Fig. 3. CVs (a) bare GCE, (b) CS/GCE, (c) AuNPs@PANI/CS/GCE in 0.1 M PBS pH 6.0 at a scan rate of 50 mV s^{-1}.

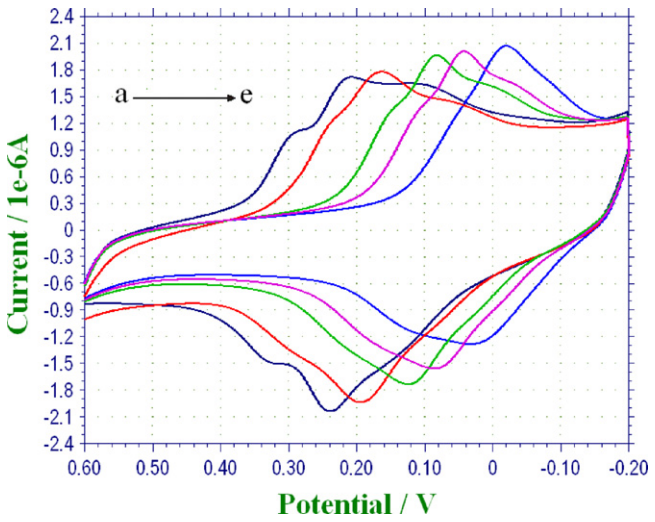

Fig. 4. CVs of the AuNPs@PANI/CS/GCE in 0.1 M PBS at pH (a) 5.0; (b) 6.0; (c) 7.0; (d) 8.0; (e) 9.0 at a scan rate of 50 mV s^{-1}.

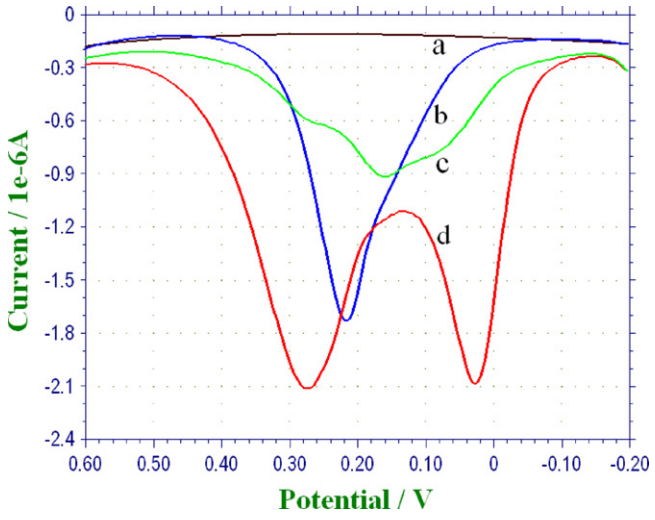

Fig. 5. DPVs of bare GCE (a and b) and AuNPs@PANI/CS/GCE (c and d) in 0.1 M PBS (pH 6.0) in the presence (b and d) and absence (a and c) of 2.0×10^{-4} M DA and 1.5×10^{-4} M AA at a scan rate of 50 mV s^{-1}.

electron transfer resistance (*R*et) were observed upon the stepwise modification of the electrode. Compared with bare GCE (Fig. S1(a)), CS/GCE showed a smaller electron transfer resistance (*R*et) value (Fig. S1(b)). This could be understood that a positively charged surface of CS formed on GCE promotes the diffusion of $Fe(CN)_6^{3-/4-}$ towards the electrode surface. However, the plot of AuNPs@PANI/CS/GCE was almost a straight line (Fig. S1(c)), indicating that AuNPs@PANI nanocomposites were excellent electric conducting composites and accelerated the electron transfer.

The electroactivity of AuNPs@PANI nanocomposites is investigated in 0.1 M PBS with various pH values ranging from 5.0 to 9.0. Generally, PANI is redox–active only for acid media with pH <4 [19,20]. As shown in Fig. 4, two pairs of redox peaks of AuNPs@PANI could be observed when pH value was 5.0. These two pairs of peaks merged and showed only one pair of broad peaks when pH value was 6. The well-defined redox peaks could be observed even when pH value was 9.0, indicating that AuNPs@PANI nanocomposites show excellent electrochemical behavior at neutral and alkalescent environment. It has been reported that PANI has three sets of redox peaks in acid media. At higher pH value, these redox peaks would merge into a broad redox peak [37–40]. Two sets of peaks of PANI correspond to the redox transitions between leucoemeraldine and emeraldine and between emeraldine and pernigraniline, respectively. Another set of peaks has also been identified as belonging to the water-soluble degradation products. In order to meet the needs of bioanalysis under physiological condition, the experiment was carried out in PBS with a pH value of 6.0

3.4. Electrochemical behaviors of AA and DA at AuNPs@PANI/CS/GCE

3.4.1. Voltammetric separation for the anodic waves of DA and AA

In order to investigate the electrocatalytic activity of the AuNPs@PANI, control experiments for the simultaneous determination of DA and AA were carried out by DPV with the bare GCE and AuNPs@PANI/CS/GCE, respectively. As shown in Fig. 5(b), the voltammetric response of the bare GCE is observed as one peak at 230 mV for the oxidation of DA and AA. The peak potentials for DA and AA were indistinguishable. Therefore, it is impossible to determine the individual concentration from the overlapped oxidation peaks. In contrast, AuNPs@PANI nanocomposites modified GCE could efficiently resolve this issue. Two defined oxidation peaks at 28, 264 mV in DPV (Fig. 5(d)) were revealed corresponding to the oxidation of AA and DA, respectively. The potential separation between two substrates was 236 mV. Such large separation allows the selective and simultaneous determination of AA and DA in their mixture.

Considering that the PANI is π-rich in nature, the π–π interaction between phenyl structure of DA and PANI makes the easy arrival of DA molecules to the surface of modified electrode. Secondly, although the π–π interaction between penta-heterocycle of AA and PANI is weak, the presence of positively charged CS provides a remarkable electrostatic attraction to negatively charged AA in PBS (pH 6.0) due to the charge characteristic of AA ($pK_a = 4.10$). The integrated effect of the above aspects might result in simultaneous determination of DA and AA at the AuNPs@PANI-modified GCE electrode.

3.4.2. Selective determination of AA and DA

To verify the feasibility of the simultaneous determination of DA and AA at AuNPs@PANI/CS/GCE, the DPVs carried out at AuNPs@PANI/CS/GCE in solutions containing various concentrations of DA and 0.1 mM AA have been illustrated in Fig. S2 (see supplementary material Fig. S2). The peak current response for the oxidation of DA linearly increases with the increase of DA concentration, while the peak current for AA oxidation keeps nearly unchanged. This demonstrates that AA has no interference for the detection of DA. Similarly, with the increase of AA concentration, the oxidation current of AA exhibits a linear increase (see supplementary material Fig. S3), which suggests that the presence of DA does not interfere with the response of AA oxidation. The peak currents for DA and AA increased linearly with correlation coefficients of 0.9997 and 0.9998 respectively, while increasing their concentrations (10–1500 μM for DA and 20–1400 μM for AA). All the results strongly imply that DA and AA can be separately determined in their mixture using the proposed method.

3.4.3. Simultaneous determination of DA and AA

To further investigate the applicability of AuNPs@PANI/CS/GCE for the simultaneous determination of both analytes in a mixture, the current responses of these species by simultaneously changing the concentrations of DA and AA have been measured. As depicted in Fig. 6, the peak currents for DA and AA increased linearly with correlation coefficients of 0.9997 and 0.9998 respectively, while increasing their concentrations (10–1700 μM for DA and 20–1600 μM for AA). The relative standard deviations for DA

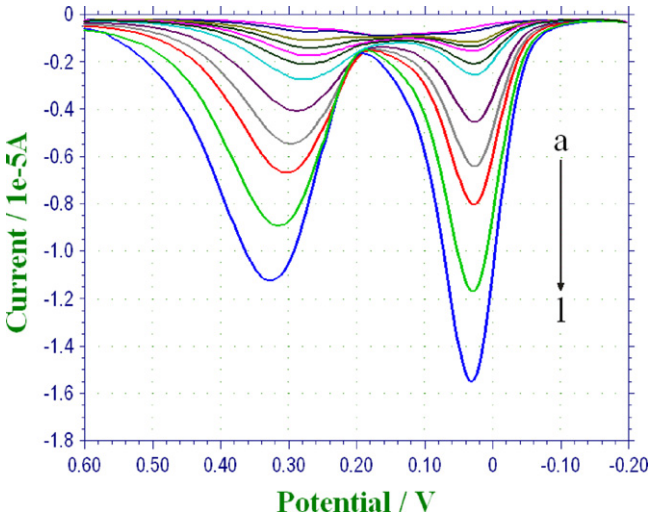

Fig. 6. DPVs of AuNPs@PANI/CS/GCE in 0.1 M PBS pH 6.0 containing different concentrations of DA and AA. DA concentrations from (a) to (l) are: 0, 10, 50, 100, 150, 200, 300, 500, 700, 900, 1300 and 1700 μM; AA concentrations from (a) to (l) are: 0, 20, 60, 80, 100, 150, 200, 400, 600, 800, 1200 and 1600 μM. Scan rate: 50 mV s^{-1}.

and AA based on eight times measurements in the mixture of 100 μM DA and 100 μM AA are 3.3% and 4.5%, respectively.

In order to demonstrate the analytical capacity of the proposed biosensor, a comparison of linear range and low detection limit with other electrode for the determination of AA and DA was listed in Table S1. Compared with the sensor based on poly(acriflavine) [S1], iodine–adlayer [S2] and poly(4-aminothiophenol)/Au_{nano} [S4], the proposed method shows a more wide liner range of detection for AA and DA. Even though the detection limit of current proposed biosensor is comparable or a little higher than that reported in the reference, the AuNPs@PANI nanocomposites modified electrode provide a very well platform for the simultaneous determination of AA and DA. The good electroactivity of AuNPs@PANI nanocomposites also shows a huge potential for the fabrication of other sensors or biosensors.

3.5. Reproducibility and stability of the biosensor

The reproducibility and stability of the developed biosensor were also investigated. The relative standard deviation (R.S.D.) for DA and AA of the 3.2% and 3.5% were obtained for the sensor response to 0.1 mM DA and AA for the same electrode with continuously testing for 30 times. The storage stability of the sensor was examined by intermittently measuring the current response to DA and AA standard solution every 3 days over the period of a month. The response could maintain about 86% of its original response after one month. Thus, the DA and AA sensor showed a good stability and reproducibility for the determination of DA and AA.

3.6. Analytical application

In order to verify the practicability of the proposed biosensor for analysis of DA and AA, the modified electrode was applied to determine DA and AA in human serum. The serum samples were diluted 10 times with PBS and different amounts of DA and AA were added without further treatment. Then, 5.0 mL of the sample solution was transferred into the electrochemical cell for the determination of these analytes using DPV. For DA determination, the recoveries ranged from 98.2% to 106.5%. For AA determination, the recoveries ranged from 98.8% to 104.5% (Table S2). The good recoveries indicate that the proposed method has potential application for the determination of DA and AA in commercial samples.

4. Conclusions

AuNPs@PANI core–shell nanocomposites were successfully prepared by one-step chemical oxidative polymerization of aniline using $HAuCl_4$ as the oxidant and AuNPs as seeds in the presence of sodium dodecyl sulfate. Due to the excellent electrochemical behavior of AuNPs@PANI in neutral and even in alkaline media, it is very suitable for sensing the species in biological fluids in physiological condition. The AuNPs@PANI/CS/GCE showed excellent catalytic activity towards the electro-oxidation of AA and DA and could be used for the simultaneous determination of AA and DA in their binary mixture. The proposed method has also been applied for detecting DA and AA in real samples with satisfactory results.

Acknowledgements

This research was supported by the National Natural Science Foundation of China (Nos. 21175076 and 21005043), the National Key Technology R&D Program (2010BAC69B01), the Scientific Special Expenditure for Non-profit Public Industry of State Oceanic Administration (201105020), the Science Foundation of Shandong Province Postdoctor (No. 200902013), and the Basic Research Program of Qingdao (No. 11-2-4-3-(4)-jch).

Appendix A. Supplementary data

Supplementary data associated with this article can be found, in the online version, at doi:10.1016/j.talanta.2011.12.002.

References

[1] R.M. Wightman, L.J. May, A.C. Michael, Anal. Chem. 60 (1988) 769–779.
[2] J.W. Mo, B. Ogorevc, Anal. Chem. 73 (2001) 1196–1202.
[3] I. Koshiishi, T. Imanari, Anal. Chem. 69 (1997) 216–220.
[4] R.D. O'Neill, Analyst 119 (1994) 767–779.
[5] Z.Q. Gao, H. Huang, Chem. Commun. 19 (1998) 2107–2108.
[6] J.S. Huang, Y. Liu, H. q. Hou, T.Y. You, Biosens. Bioelectron. 24 (2008) 632–637.
[7] D. Ragupathy, A.I. Gopalan, K.P. Lee, Sens. Actuators B: Chem. 143 (2010) 696–703.
[8] A. Stoyanova, S. Ivanova, V. Tsakova, A. Bund, Electrochim. Acta 56 (2011) 3693–3699.
[9] R. Manjunatha, G.S. Suresh, J.S. Melo, S.F. D'Souza, T.V. Venkatesha, Sens. Actuators B: Chem. 145 (2010) 643–650.
[10] F. Li, C.F. Tang, S.F. Liu, G.R. Ma, Electrochim. Acta 55 (2010) 838–843.
[11] A.I. Gopalan, K.P. Lee, K.M. Manesh, P. Santhosh, J.H. Kim, J.S. Kang, Talanta 71 (2007) 1774–1781.
[12] F. Li, L.M. Yang, C. Zhao, Z.F. Du, Anal. Methods 3 (2011) 1601–1606.
[13] P. Kalimuthu, S.A. John, Talanta 80 (2010) 1086–1091.
[14] K. Amano, H. Ishikawa, A. Kobayashi, M. Satoh, E. Hasegawa, Synth. Met. 62 (1994) 229–232.
[15] S.A. Kumar, S.F. Wang, T.C.K. Yang, C.T. Yeh, Biosens. Bioelectron. 25 (2010) 2592–2597.
[16] Y.G. Liu, X.M. Feng, J.M. Shen, J.J. Zhu, W.H. Hou, J. Phys. Chem. B 112 (2008) 9237–9242.
[17] H.G. Xue, Z.Q. Shen, Talanta 57 (2002) 289–295.
[18] Y.F. Hu, Z.H. Zhang, H.B. Zhang, L.J. Luo, S.Z. Yao, Talanta 84 (2011) 305–313.
[19] A.F. Diaz, J.A. Logan, J. Electroanal. Chem. 111 (1980) 111–114.
[20] H.A. Zhong, R. Yuan, Y.Q. Chai, W.J. Li, X. Zhang, Y. Zhang, Talanta 85 (2011) 104–111.
[21] S.J. Tian, A. Baba, J.Y. Liu, Z.H. Wang, W. Knoll, M.K. Park, R. Advincula, Adv. Funct. Mater. 13 (2003) 473–479.
[22] S. Virji, J. Huang, R.B. Kaner, B.H. Weiller, Nano Lett. 4 (2004) 491–496.
[23] B.A. Deore, M.S. Freund, Macromolecules 42 (2009) 164–168.
[24] Y.H. Tang, K.X. Pan, X.J. Wang, C.B. Liu, J. Electroanal. Chem. 639 (2010) 123–129.
[25] T.K. Sarma, D. Chowdhury, A. Paul, A. Chattopadhyay, Chem. Commun. 2 (2002) 1048–1049.
[26] Q. Xu, J. Leng, H.B. Li, G.J. Lu, Y. Wang, X.Y. Hu, React. Funct. Polym. 70 (2010) 663–668.
[27] Y. Wang, Z.M. Liu, B.X. Han, Z.Y. Sun, Y. Huang, G.Y. Yang, Langmuir 21 (2005) 833–836.
[28] Z.J. Wang, J.H. Yuan, D.X. Han, Y.J. Zhang, Y.F. Shen, D. Kuehner, L. Niu, A. Ivaska, Cryst. Growth Des. 8 (2008) 1827–1832.
[29] S.X. Xing, L.H. Tan, M.X. Yang, M. Pan, Y.B. Lv, Q.H. Tang, Y.H. Yang, H.Y. Chen, J. Mater. Chem. 19 (2009) 3286–3291.

[30] Z.Q. Peng, L.M. Guo, Z.H. Zhang, B. Tesche, T. Wilke, D. Ogermann, S.H. Hu, K. Kleinermanns, Langmuir 22 (2006) 10915–10918.
[31] A. Doron, E. Katz, I. Willner, Langmuir 11 (1995) 1313–1317.
[32] J.J. Xu, X.L. Luo, Y. Du, H.Y. Chen, Electrochem. Commun. 6 (2004) 1169–1173.
[33] K.C. Grabar, R.G. Freeman, M.B. Hommer, M.J. Natan, Anal. Chem. 67 (1995) 735–743.
[34] Y. Cao, P. Smith, A. Heeger, J. Synth. Met. 32 (1989) 263–281.
[35] E. Granot, E. Katz, B. Basnar, I. Willner, Chem. Mater. 17 (2005) 4600–4609.
[36] R. Ehret, W. Baumann, M. Brischwein, A. Schwinde, K. Stegbauer, B. Wolf, Biosens. Bioelectron. 12 (1997) 29–41.
[37] Y. Wei, W.W. Focke, G.E. Wnek, J. Phys. Chem. 93 (1989) 495–499.
[38] W.W. Focke, G.E. Wnek, Y. Wei, J. Phys. Chem. 91 (1987) 5813–5818.
[39] M.K. Park, K. Onishi, J. Locklin, F. Caruso, R.C. Advincula, Langmuir 19 (2003) 8550–8554.
[40] S.J. Tian, A. Baba, J.Y. Liu, Z.H. Wang, W. Knoll, M.K. Park, R. Advincula 13 (2003) 473–478.